Effect of Fungal Death or Inhibition Induced by Oxycarboxin or Polyoxin D on the Interaction between Resistant or Susceptible Bean Cultivars and the Bean Rust Fungus

Michèle C. Heath

Professor, Botany Department, University of Toronto, Ontario M5S IAI, Canada.
The technical assistance of L. Babcock and K. Sault is gratefully acknowledged.
Accepted for publication 27 June 1988 (submitted for electronic processing).

ABSTRACT

Heath, M. C. 1988. Effect of fungal death or inhibition induced by oxycarboxin or polyoxin D on the interaction between resistant or susceptible bean cultivars and the bean rust fungus. Phytopathology 78:1454-1462.

Light and electron microscopy of resistant or susceptible bean leaves inoculated with the bean rust fungus and then treated with the fungicide oxycarboxin or the chitin synthesis inhibitor polyoxin D confirmed that the typical plant response to the dead fungus is the encasement of haustoria in the absence of plant cell necrosis. In the untreated resistant cultivar, necrosis commonly was detected first in cells adjacent to those containing haustoria at about 2 days after inoculation; the chemicals inhibited such necrosis if applied 1 day after inoculation. Polyoxin D treatment at this time allowed more infection sites to develop necrotic cells than did oxycarboxin application, apparently because after treatment with the former, some haustoria remained alive and continued to grow. These results indicate that haustorium walls do not contain chitin, that only the living haustorium elicits necrosis, and that it does so a few hours after it becomes mature. Ultrastructurally, the incompatible interaction was characterized by silica deposition in plant cells next to dead ones, wide electron-opaque extrahaustorial matrices, and the widespread deposition of callose-like material along the wall of haustorium-containing cells. Polyoxin-induced fungal death in the compatible cultivar did not elicit ultrastructural features typical of the incompatible interaction except for a slight increase in electron-opaque material in the extrahaustorial matrix.

In a previous paper (7), it was reported that heat-induced death of the bean rust fungus, *Uromyces appendiculatus* (Pers.) Unger var. *appendiculatus*, resulted in the development of callose-containing encasements around the fungal haustoria in both resistant and susceptible cultivars of bean (*Phaseolus vulgaris* L.). Little or no plant cell necrosis subsequently developed in the susceptible cultivar or in the resistant one as long as the heat treatment was applied early enough after inoculation. Whereas these data suggest that the typical response of a bean leaf cell to fungal death is encasement of the haustorium rather than the plant cell death suggested by others (11), the possibility remains that the heat treatment could have influenced the plant response; moreover, heat-labile fungal products that might normally elicit necrosis could have been inactivated. Therefore, the present study was initiated to investigate how resistant and susceptible bean plants respond to fungal death, or inhibition, caused by the systemic fungicide oxycarboxin, an inhibitor of mitochondrial respiration (15), or polyoxin D, an inhibitor of chitin synthetase (3).

MATERIALS AND METHODS

Bean cultivars Pinto and 765, susceptible and resistant, respectively, to the race of the fungus used, were grown in growth chambers and inoculated after 13–14 days with urediospores of *U. appendiculatus* as described previously (7). For treatment with the fungicide, inoculated primary leaves were detached from the plant with a sharp razor blade at 22 or 46 hr after inoculation. The petiole from one leaf of each plant was immediately placed in a 250-ml flask containing 125 ml of double-distilled water, and that of the other leaf placed in 125 ml of a 40 μl/ml aqueous solution of Plantvax 2E containing 200 g/l of oxycarboxin (UniRoyal Chemicals Canada Inc.; a gift from L. Edgington). Leaves were returned to the growth chamber, and 1 cm^2 pieces were harvested 5 days after inoculation.

To examine the effect of polyoxin D, a 4×10^{-4} M aqueous solution of the inhibitor (Calbiochem-Behring Corp.) was injected (5) into the intercellular spaces of attached primary leaves at 24 or 48 hr after inoculation. For each plant, one leaf was injected with

the inhibitor and the other was injected with water. Injected leaf pieces were harvested 4 days after injection.

Leaf pieces usually were decolorized in boiling ethanol, cleared in chloral hydrate, mounted in modified Hoyer's medium, and examined under differential interference contrast (DIC) light microscopy or by epifluorescence microscopy (for autofluorescence) as described before (7). To determine the incidence of refractive mesophyll walls, duplicate samples were examined by DIC microscopy after mounting the tissue in Canada balsam (17). The total length of hyphae at each infection site was estimated with the aid of an ocular micrometer. For each leaf piece, 20–25 infection sites were examined, and for each sampling time, 1 leaf piece was cut from each of at least three plants. Each experiment was repeated twice. Mean values per treatment were calculated as the average of the values for each leaf piece. For statistical analysis, Fisher's least-significant difference test (13) was applied; arc sine transformed percentages were used where appropriate (16). Data are presented as the combined values from both experiments because no significant differences were found between them.

For electron microscopy, tissue pieces were harvested 3 days after injection of polyoxin D and from comparable plants injected with water. Leaves were injected at 24 or 48 hr after the inoculation of 13- or 14-day-old plants. The tissue was fixed in glutaraldehyde, postfixed in osmium tetroxide, dehydrated in an ethanol series, and embedded in Epon 812 as described previously (17). Serial ultrathin sections were mounted on formvar-coated, single-hole copper grids and stained with lead citrate and uranyl acetate. In some cases, thicker (blue interference color) sections were mounted on gold grids and treated with freshly prepared, 1% aqueous periodic acid for 90 min in the dark; such sections were examined unstained. All sections were examined with a Philips 201C transmission electron microscope operated at 60 kV. All measurements of the widths of haustorial walls and extrahaustorial matrices were made from micrographs in regions where the section clearly cut them perpendicularly (i.e., clear tripartite images were present for both the fungal plasmalemma and the adjacent extrahaustorial membrane).

RESULTS

Light microscopy: compatible interaction. At the time of inhibitor treatment, infection sites usually had 1-2 haustoria

(22–24 hr after inoculation) or about 4 (46–48 hr after inoculation) haustoria. Preliminary experiments showed that detaching the primary leaves within 48 hr after inoculation and placing their petioles in water had no obvious effect on subsequent fungal development. However, injecting attached leaves with water at either 24 or 48 hr after inoculation appeared to temporarily slow fungal growth so that colonies in leaf pieces harvested 48 hr later appeared slightly smaller than those in uninjected tissue. In other respects, however, fungal development and plant response appeared normal. In contrast, the similar application (at 22 or 46 hr) of oxycarboxin to detached leaves, or the injection (at 24 or 48 hr) of polyoxin D into attached leaves, caused the almost

immediate cessation of fungal growth, as witnessed by the fact that hyphal lengths recorded several days later were similar to those observed at the time of treatment (data not shown). In experimental tissue harvested 5–6 days after inoculation, almost all of the infection hyphae were strongly autofluorescent, and presumably dead (7), compared with the 12% or less of autofluorescent infection hyphae seen in the controls (Table 1). When applied 1 day postinoculation (d.p.i.), both inhibitors caused an increase (compared with control plants) in the percentage of infection sites lacking a haustorium, presumably because fungal growth at some infection sites had been inhibited before haustorium formation. Application of the inhibitors at

TABLE 1. Effect of oxycarboxin and polyoxin D supplied to compatible bean cultivar Pinto leaves after inoculation with *Uromyces appendiculatus*[w]

| | Treatment and time of application after inoculation | | | | | |
| | Oxycarboxin | | Polyoxin D | | Water[x] | |
	22 hr	46 hr	24 hr	48 hr	22–24 hr	46–48 hr
Mean hyphal length (μm)	55 a	144 b	62 a	137 b	...[z]	...
% infection sites:						
Without haustoria	29 a	17 ab	24 a	19 ab	11 b	11 b
With fluorescent IH[y]	100 a	100 a	94 b	100 a	12 c	6 c
With necrotic cells	13 a	7 a	24 a	14 a	1 b	2 b
With encased haustoria	66 a (100)	82 b (100)	42 c (100)	56 ac (100)	1 d	2 d
(% of these in nonnecrotic cells)						
Average number of necrotic cells per site	6 a	3 b	8 a	6 a	1 b	1 b
% of all haustoria:						
Detectably encased	99 a (100)	100 a (100)	62 b (85)	52 b (81)	...	...
(% of these fluorescent)						
With many lobes	0 a	0 a	24 b (7)	32 b (62)	...	...
(% of these fluorescent)						

[w]Tissue was harvested 5–6 days after inoculation. Values represent combined data from two experiments; those in each row followed by the same letter are not significantly different at $P = 0.5$ (Fisher's least significant difference).
[x]Combined values from water controls of detached and undetached leaves.
[y]IH = infection hypha.
[z]... = not determined.
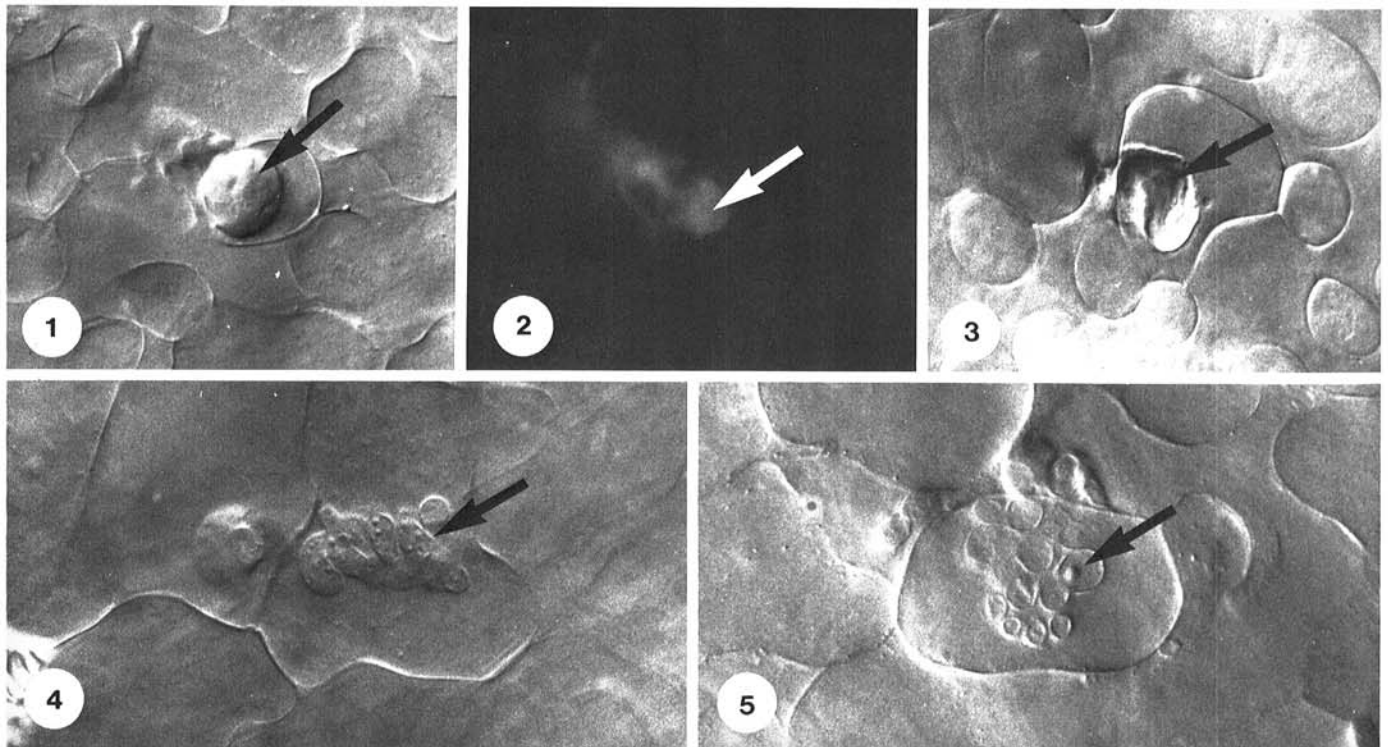
Figs. 1–5. Compatible interaction seen by light microscopy of whole mounts of cleared leaves. **1,** Oxycarboxin applied at 1 day postinoculation (d.p.i.), tissue harvested at 6 d.p.i. Encased haustorium (arrow) in a nonnecrotic cell ($\times$ 739). **2,** Autofluorescence of the haustorium (arrow) shown in Figure 1 ($\times$ 739). **3,** Polyoxin D applied 1 d.p.i., tissue harvested 6 d.p.i. Encased haustorium (arrow) in a nonnecrotic cell ($\times$ 739). **4,** Polyoxin D applied at 2 d.p.i., tissue harvested at 7 d.p.i. Large haustorium (arrow) with interwoven lobes in a nonnecrotic cell ($\times$ 819). **5,** Control, infected tissue harvested 7 d.p.i. Large, lobed, first-formed haustorium (arrow) at the center of a growing colony ($\times$ 819).

either 1 or 2 d.p.i. resulted in more infection sites with necrotic cells (as detected by browning or autofluorescence) (7) than were seen in the water controls, but in no instance did the mean value exceed 24%.

In oxycarboxin-treated tissue, almost all of the detectable haustoria appeared encased (Fig. 1) and autofluorescent (Fig. 2) by the time of harvest, regardless of when the inhibitor was applied. The cells containing these haustoria appeared normal and did not autofluoresce. Only a very few sites were observed where unencased haustoria were seen in necrotic cells. In contrast, although over half of the haustoria seen in polyoxin D-treated tissue were encased and in apparently nonnecrotic cells (Fig. 3), about a quarter appeared not to be encased. The bodies of these haustoria were not the usual spherical shape typical of encased haustoria, but were larger, with many interwoven finger-like lobes (Fig. 4). In appearance, these haustoria closely resembled older haustoria seen at the center of large, healthy colonies formed in untreated, intact plants or in the water controls (Fig. 5). Many of the lobed haustoria in polyoxin-treated tissue appeared nonnecrotic and did not autofluoresce.

As bean leaves age, inoculation with the bean rust fungus results in an increasing percentage of infection sites at which the infection hypha fails to form the first haustorium (6). This lack of haustoria correlates with the presence of silica deposits on and in the mesophyll wall (6), and such deposits can be detected by light microscopy by their high refractivity when the tissue is mounted in Canada balsam (17). To see if such deposits were induced by the previous death of the infection hypha, the incidence of refractive plant walls at infection sites lacking haustoria was examined in tissue treated with water or with oxycarboxin 22 hr after inoculation. Relatively few infection sites lacking haustoria were seen in each leaf piece, so the data from all leaf pieces were combined. Whereas refractive mesophyll walls were seen at all haustorium-lacking sites in the control tissue (n = 20), only 21% of

such sites (n = 138) in oxycarboxin-treated tissue had refractive walls. In contrast, autofluorescent mesophyll walls were seen in cleared tissue at 62% of haustorium-lacking sites (n = 78) in oxycarboxin-treated tissue and at 96% of such sites (n = 26) in water-treated leaves.

Light microscopy: incompatible interaction. A preliminary investigation revealed no discernable differences in fungal development or plant response in cleared pieces of untreated leaves, attached leaves injected with water at 24 or 48 hr after inoculation, or leaves detached at 22 or 46 hr after inoculation and incubated with their petioles in water. In all cases, fungal development resembled that in the compatible cultivar until at least 30 hr after inoculation, and no autofluorescence or browning of invaded or adjacent mesophyll cell contents could be detected. However, necrotic (i.e., with autofluorescent and browning contents) mesophyll cells were observed at about 30% of infection sites at 48 hr after inoculation (somewhat earlier than in previous experiments) (7). Careful examination revealed that in about 50% of these sites, it was the cells surrounding the cell containing the first-formed haustorium that were necrotic (Figs. 6 and 7). By 72 hr after inoculation, all haustorium-containing infection sites contained several brown, autofluorescent cells (mostly without haustoria), sometimes surrounded by nonnecrotic cells with autofluorescent walls. Fungal growth usually ceased between 72 and 96 hr after inoculation (7), and most infection sites subsequently could be identified as a small patch of collapsed, dark brown mesophyll cells in which the fungus was not clearly discernible. However, a few colonies continued to grow, resulting in a large mycelium with normal-appearing haustoria; necrotic cells were either interspersed throughout the infected area or localized to a patch on one side from which the fungus appeared to have "escaped."

In tissue treated with oxycarboxin at 22 hr after inoculation, data collected from tissue harvested and cleared 4 days later (Table
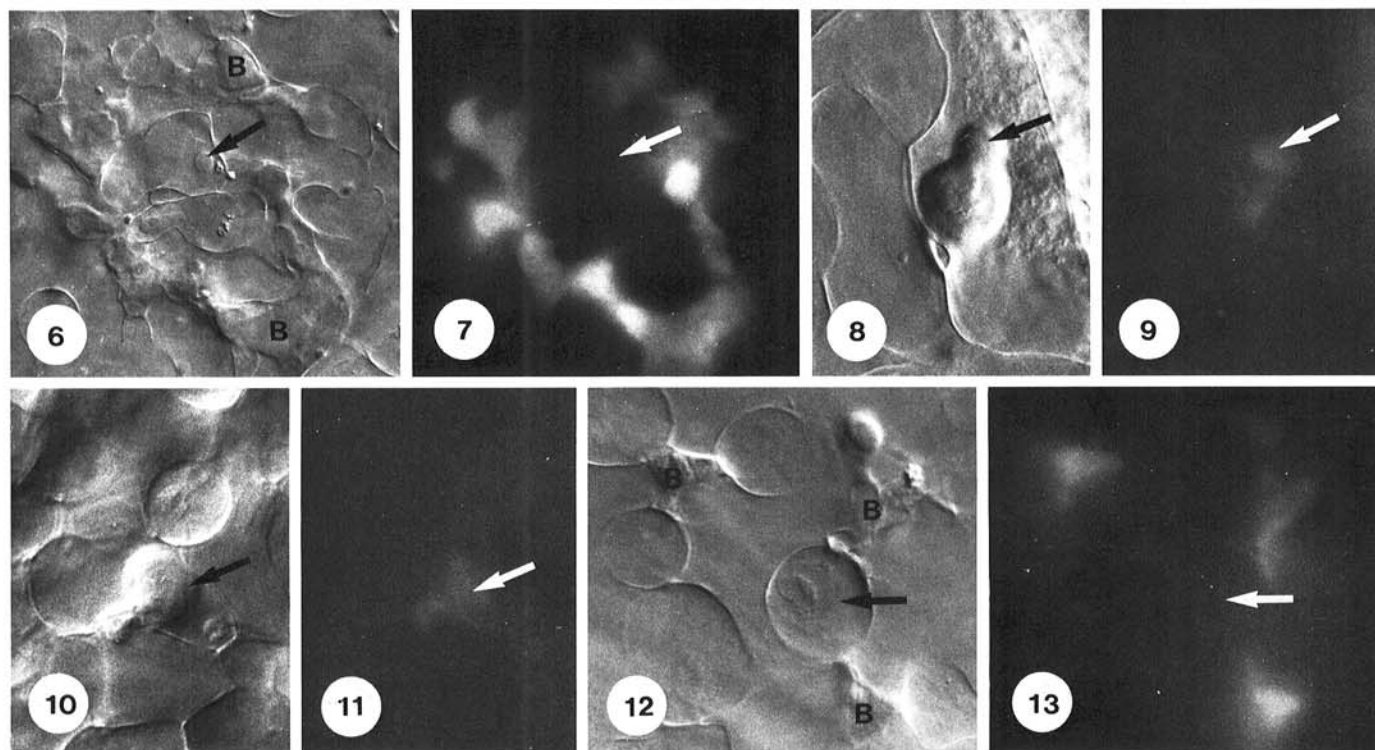
Figs. 6–13. Incompatible interaction as seen by light microscopy of whole mounts of cleared leaves. **6,** Untreated tissue, 2 d.p.i. The infection site contains a haustorium (arrow) in a nonnecrotic cell, and several collapsed brown cells (B) (× 703). **7,** Autofluorescence of the necrotic cells shown in Figure 6. Note that the haustorium-containing cell (arrow) is not autofluorescent (× 703). **8,** Oxycarboxin applied at 1 d.p.i., tissue harvested at 6 d.p.i. The infection site contains a single encased haustorium (arrow) and no necrotic cells (× 783). **9,** Autofluorescence of the haustorium (arrow) shown in Figure 8 (× 783). **10,** Polyoxin D applied at 1 d.p.i., tissue harvested at 4 d.p.i. The infection site contains one encased haustorium (arrow) and no necrotic cells (× 863). **11,** Autofluorescence of the haustorium (arrow) shown in Figure 10 (× 863). **12,** Polyoxin D applied at 1 d.p.i., tissue harvested at 4 d.p.i. An infection site with an unencased haustorium (arrow) in a nonnecrotic cell. Note the surrounding brown, collapsed cells (B) (× 783). **13,** Autofluorescence of the collapsed cells shown in Figure 12. Note that the haustorium-containing cell (arrow) is not autofluorescent (× 783).

2) closely resembled that from similarly treated susceptible tissue (compare Tables 1 and 2). About one-third of all infection sites lacked haustoria, presumably because the fungus was inhibited before haustorium formation. All infection hyphae were autofluorescent, but only 17% of infection sites had necrotic cells. At some of these sites, and at all other sites, haustoria were autofluorescent, encased, and in nonnecrotic cells (Figs. 8 and 9). In contrast, more than 80% of infection sites had necrotic cells in tissue treated with the fungicide at 46 hr after inoculation. Encased haustoria in nonnecrotic cells could be discerned at about one-quarter of these sites, whereas such haustoria were seen in only 1% of infection sites in control tissue. At the remaining sites, all cells in the infected area were brown, and haustoria could not be detected with certainty. The average number of necrotic cells at sites with necrosis was about twice that seen in tissue given the fungicide at 22 hr and similar to that in the water controls.

Data from tissue injected with polyoxin D differed from those from oxycarboxin-treated leaves in several ways. Infection hyphae were not all autofluorescent (and presumably dead) by the time of tissue harvest, and about a third of the observed haustoria in tissue treated at 24 hr were large, unencased, and lobed (Table 2). Only about one-half of these haustoria were autofluorescent, compared with virtually all of those haustoria that were visibly encased (Figs. 10 and 11). In addition, for tissue injected with polyoxin D at 24 hr, the number of infection sites with necrotic mesophyll cells was twice that of sites in tissue treated with oxycarboxin at 22 hr. Most of these necrotic sites contained lobed, nonfluorescent haustoria in nonfluorescent plant cells (Figs. 12 and 13).

Electron microscopy: compatible interaction. Only 1 infection site from water-injected tissue was examined, because similar sites have been observed previously (Heath, unpublished) and always seemed identical to those in untreated tissue. At this one site, no unusual responses were seen in cells surrounding the infection hypha, and seven healthy-looking haustoria were seen at various stages of development. The youngest was a haustorial neck that had not yet formed a body, around which there was a large accumulation of rough endoplasmic reticulum (ER) (Fig. 14). ER was less abundant around older haustoria, although the neck was usually ensheathed in what appeared to be a single, fenestrated ER cisterna. A large, multi-lobed haustorium, presumed by its position and size to be the first-formed haustorium, was observed at the center of the colony in a plant cell with abnormally large mitochondria (Fig. 15). One additional haustorium was observed that seemed slightly collapsed and had unusually electron-opaque contents. This haustorium was surrounded by small vesicles (confirmed as vesicles by serial section analysis) with an electron-

opaque central core, in addition to profiles of ER (Fig. 16). Some of these vesicles were in membrane continuity with the extrahaustorial membrane and did not appear to arise from the Golgi apparatus because vesicles clustered around Golgi bodies lacked an electron-opaque core. No collars or encasements of callose-like material (12) were observed associated with any haustorium. Walls of all haustoria were about 50 nm thick, except for that of the large central haustorium, which was about 100 nm wide. All haustoria were surrounded by an irregular, electron-translucent extrahaustorial matrix (EHM) that varied in thickness from about 50 to 80 nm.

Two infection sites, each with one haustorium, were examined in tissue injected with polyoxin D at 24 hr after inoculation. In both cases, the infection hypha was collapsed and had disorganized electron-opaque contents. Both infection hyphae were embedded in electron-opaque material where they touched the plant wall (Fig. 17); this material closely resembled fungal cytoplasm, but no breach in the fungal wall was observed. At one site, the haustorial mother cell (HMC) and the large haustorium were collapsed and had disorganized, electron-opaque contents (Figs. 18 and 19). The haustorial wall was about 50 nm thick, and the surrounding EHM was similar in width and appeared slightly electron-opaque (in contrast to the electron-translucent matrices seen in untreated tissue) and sometimes difficult to differentiate from the fungal wall. The haustorium was partially encased in electron-translucent, callose-like material that was separated from the haustorium by two membranes that represented the host plasmalemma lining the inside of the encasement and the evaginated part of the same membrane that covered the surface of the haustorium (12). The plasmalemma covering the outer surface of the encasement often was evaginated into, or associated with, large vesicles, some of which contained fibrillar material (Fig. 19). Similar vesicles were observed in the cytoplasm, sometimes in apparent continuity with the ER.

At the second site (Fig. 20), the HMC and the haustorial cytoplasm appeared similar to that of a large, mature haustorium typically seen in control tissue. However, the EHM contained more flocculent, electron-opaque material (Fig. 21) and was wider, varying in width from 60 to 150 nm. The haustorial wall was also thicker and ranged from 80 to 100 nm. The haustorial neck was encased in a callose-like collar (Fig. 20). As in the first infection site, the host plasmalemma covering the cytoplasm side of this callose-like material was evaginated into irregular, fibrillar-containing vesicles whose membranes more closely resembled the ER in appearance than did the rest of the membrane apressed to the collar. Vesicles similar to those seen adjacent to one of the

TABLE 2. Effect of oxycarboxin and polyoxin D supplied to incompatible bean cultivar 765 leaves after inoculation with *Uromyces appendiculatus*[v]

	Treatment and time of application after inoculation					
	Oxycarboxin		Polyoxin D		Water[w]	
	22 hr	46 hr	24 hr	48 hr	22–24 hr	46–48 hr
Mean hyphal length (μm)	56 a	...[y]	55 a	...	...	...
% infection sites:						
Without haustoria	35 a	12 b	19 b	11 b	14 b	9 b
With fluorescent IH[x]	100 a	100 a	98 b	85 b	78 b	43 c
With necrotic cells	17 a	86 b	44 c	97 b	85 b	90 b
With encased haustoria	59 a (90)	26[z]	34 b (81)	11[z]	0 c	1 c
(% of these in nonnecrotic cells)						
Average number of necrotic cells per site	4 a	9 b	5 a	13 b	12 b	9 b
% of all haustoria:						
Detectably encased	88 a (100)	...	70 b (91)	...	...	...
(% of these fluorescent)						
With many lobes	0 a	...	31 b (44)	...	...	...
(% of these fluorescent)						

[v] Tissue was harvested 5–6 days after inoculation. Values represent combined data from two experiments; those in each row followed by the same letter are not significantly different at P = 0.5 (Fisher's least significant difference).
[w] Combined values from water controls of detached and undetached leaves.
[x] IH = infection hypha.
[y] ... = not determined.
[z] Underestimates due to masking by brown cell contents.

haustoria in control tissue were present in the host cytoplasm (Figs. 21 and 22) and sometimes were seen in membrane continuity with the extrahaustorial membrane (Fig. 21). These vesicles were often aggregated in chains and were associated with tubules containing granular material (Fig. 22) and, sometimes, a central darker core.

Two infection sites were examined in tissue injected with polyoxin D at 48 hr after inoculation. At both, the intercellular mycelium and all haustoria were collapsed and contained disorganized, electron-opaque contents. At one site, 3 of the 4 haustoria had conspicuously thicker walls (100–140 nm in width) (Fig. 23) than those seen in control tissue, and all haustoria at both sites were surrounded by a slightly electron-opaque EHM (30–70 nm in width). Two haustoria at this site were partially encased, and two were associated with vesicles and tubules in the plant cytoplasm as described above. Crystalline material (Fig. 24) was observed in the vacuole of one haustorium-containing cell at each infection site.

Electron microscopy: incompatible interaction. Four infection sites were sectioned from control-inoculated tissue harvested 4 d.p.i. (Figs. 25–27, 29–31) and one infection site from tissue harvested at 5 d.p.i. (Fig. 28). This last infection site contained a fungal colony with at least seven haustoria and seemed to be a representative of the few, necrosis-lacking infection sites described above from tissue observed by light microscopy. Haustorial walls were 50–60 nm thick as in susceptible tissue and were surrounded by an EHM 50–80 nm wide containing small amounts of electron-opaque material (Fig. 28). The ultrastructure of both the fungus and the host cells also were similar to that seen in the compatible interaction except that there was extensive deposition of electron-opaque material in and on the mesophyll cell walls adjacent to the infection hypha (Fig. 25). These deposits were identical to those previously shown to contain silica (4), and they similarly retained their electron opacity after osmium was removed from unstained sections by periodic acid (19) (Fig. 27). Such deposits usually were coated with more translucent, callose-like material, and the adjacent plant plasmalemma frequently bore irregular, electron-opaque, lipid-like globules. Their lipid nature was further supported by the fact that they etched out of the section during periodic acid treatment (Fig. 27).

At the remaining four infection sites examined in control tissue,
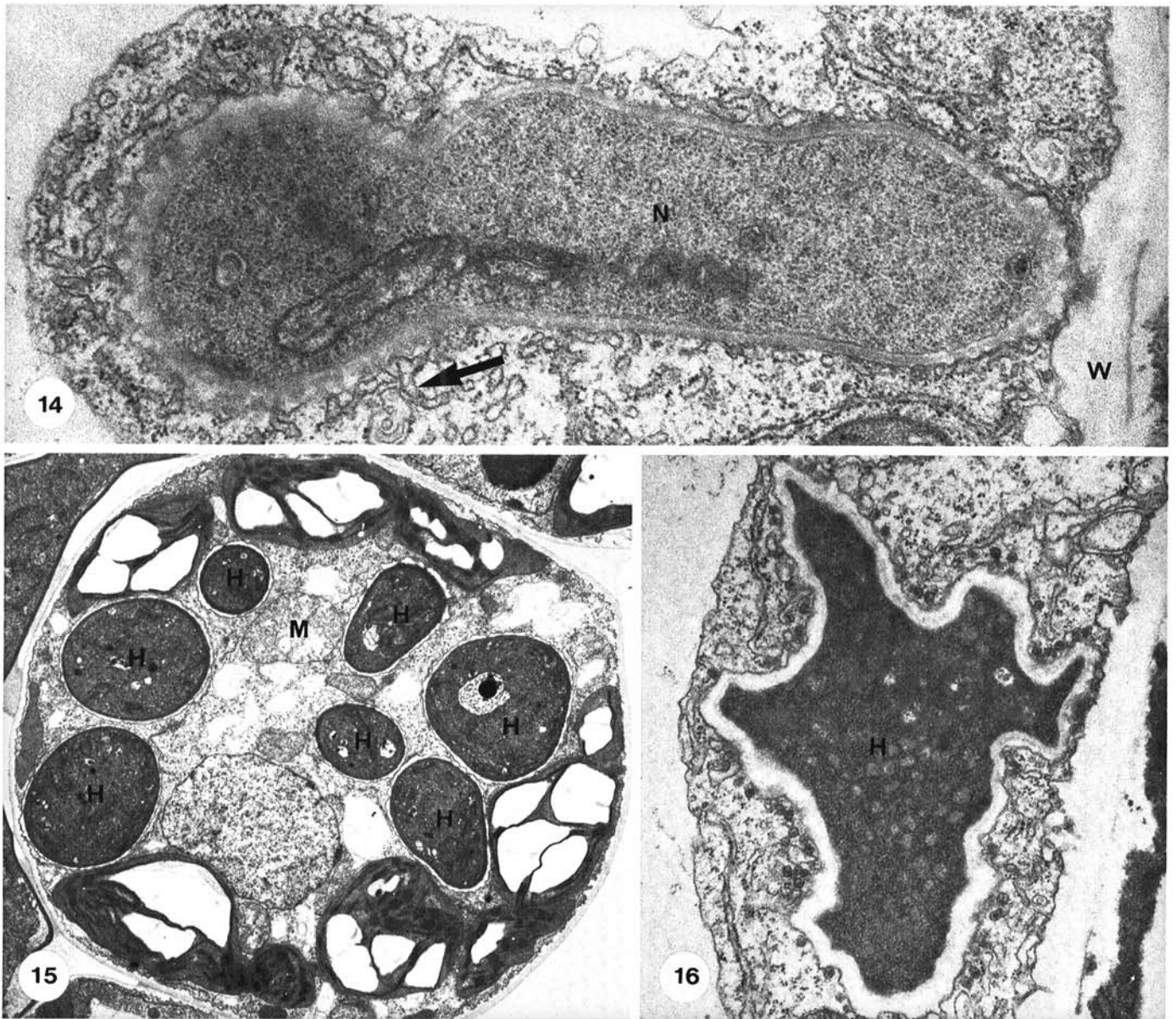
Figs. 14–16. Electron micrographs of the compatible interaction. Tissue injected with water at 1 d.p.i., harvested at 4 d.p.i. **14,** Median section through a haustorial neck (N) that has not yet formed a body. Note the accumulation of endoplasmic reticulum (arrow) in the adjacent plant cytoplasm and the absence of a neckband. The penetration peg that traverses the plant wall (W) is in an adjacent section (× 28,670). **15,** Lobes (H) of the first-formed haustorium observed at the center of the colony. Note that one of the mitochondria (M) is unusually large (c.f. Fig. 20) (× 4,090). **16,** A slightly collapsed haustorium (H) with unusually electron-opaque contents. Note the accumulation of small vesicles in the plant cytoplasm surrounding the haustorium (× 20,850).

fungal growth was much less extensive. Only 2–4 haustoria were observed per site, and each site contained 4–5 uninvaded, collapsed mesophyll cells with disorganized, electron-opaque contents. Silica deposits were seen next to the infection hypha at only one site, and all the infection hyphae appeared to contain organized cytoplasm, despite the fact that each was collapsed and vacuolate. Although most portions of the intercellular mycelium looked ultrastructurally normal (i.e., as in the compatible interaction), only one or two haustoria appeared alive at any site. These haustoria were large, possessed neckbands (12), and were in normal or slightly disorganized mesophyll cells. Haustorial walls were slightly thicker (60–100 nm in width) than in the compatible

interaction and were surrounded by an EHM 80–120 nm wide containing flocculent, electron-opaque material (Fig. 29). The remaining haustoria had disorganized cytoplasm, as did the invaded cell. In 50% (4/8) of these invaded cells, the haustorium appeared at a lesser state of degeneration than the plant cell (Fig. 30). All invaded cells that were still ultrastructurally normal, or showed only a slight degree of cytoplasmic degeneration, were lined along their cell walls with callose-like material (Fig. 29). Living cells that abutted dead invaded or uninvaded cells had similar callose-like deposits where the two cells touched. Only in one instance was silica associated with these deposits, and this was the only situation where the adjacent plant plasmalemma was
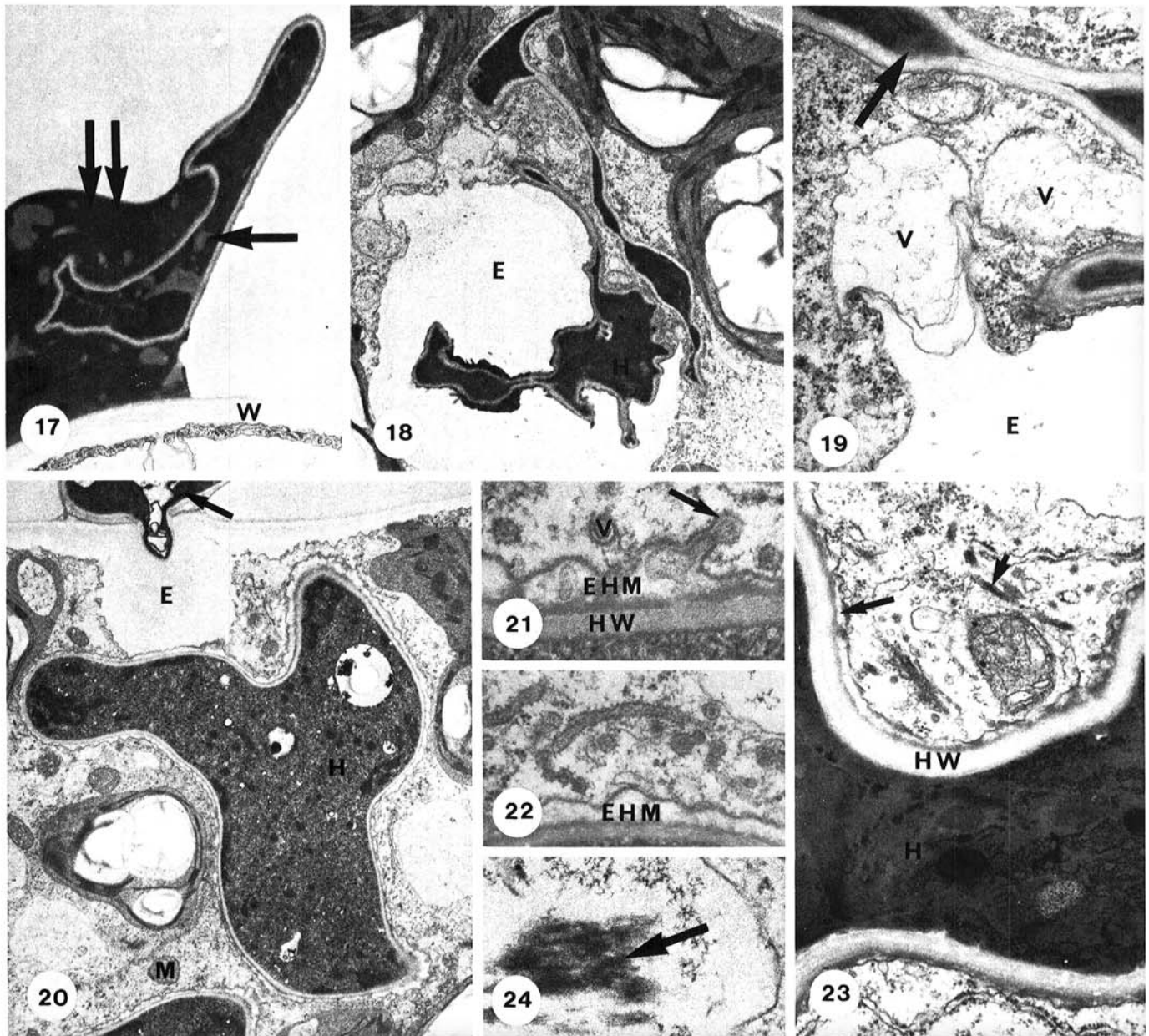
Figs. 17–24. Electron micrographs of the compatible interaction treated with polyoxin D at 1 or 2 d.p.i. and harvested at 5 d.p.i. **17,** polyoxin D applied at 1 d.p.i. Necrotic infection hypha (single arrow) embedded in electron-opaque material (double arrow) near the wall (W) of a mesophyll cell (× 10,634). **18,** Polyoxin D applied at 1 d.p.i. Collapsed haustorium (H), with electron-opaque contents, that is partially encased in callose-like material (E) (× 5,970). **19,** Detail of the cell shown in Figure 18, showing large vesicles (V) with fibrillar contents adjacent to the encasement (E) and haustorium (arrow) (× 25,520). **20,** Polyoxin D applied at 1 d.p.i. Infection site in which the haustorium (H) is not necrotic, but its neck is encased in a collar (E) of callose-like material. The haustorial mother cell (arrow) appears normal, as does the host-cell cytoplasm, including the mitochondria (M) (× 4,950). **21,** Detail of part of the extrahaustorial matrix (EHM) adjacent to the wall (HW) of the haustorium shown in Figure 20. Note the vesicles (V) in the adjacent host cytoplasm and the apparent continuity between the membrane of one of these vesicles (arrow) and the extrahaustorial membrane (× 47,760). **22,** Another region of the extrahaustorial matrix (EHM) surrounding the haustorium shown in Figure 20. Note the tubules and vesicles (some in chains) in the host cytoplasm (× 29,850). **23,** Polyoxin D applied at 2 d.p.i. A necrotic haustorium (H) surrounded by a thick haustorial wall (HW) and a relatively narrow extrahaustorial matrix (long arrow). Note the tubules (short arrow) and vesicles in the surrounding host cytoplasm (× 27,500). **24,** An inclusion (arrow) in the vacuole of the plant cell illustrated in Figure 23 (× 45,990).
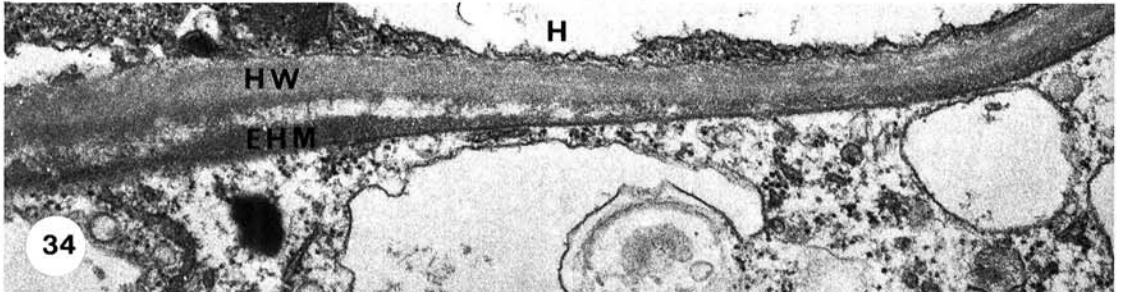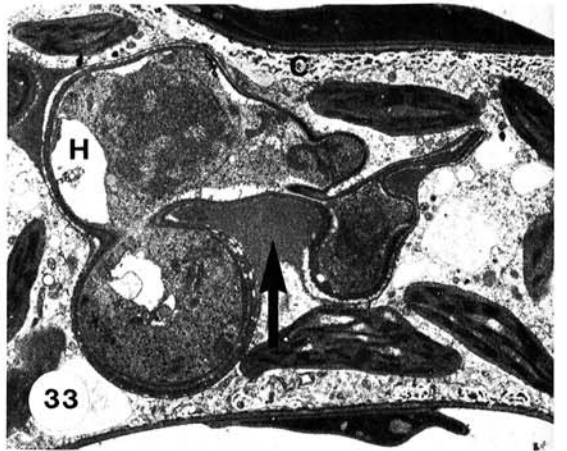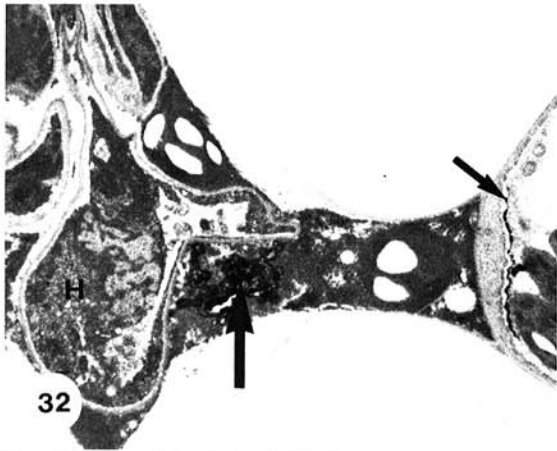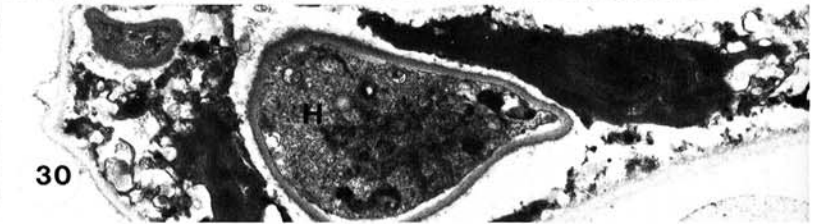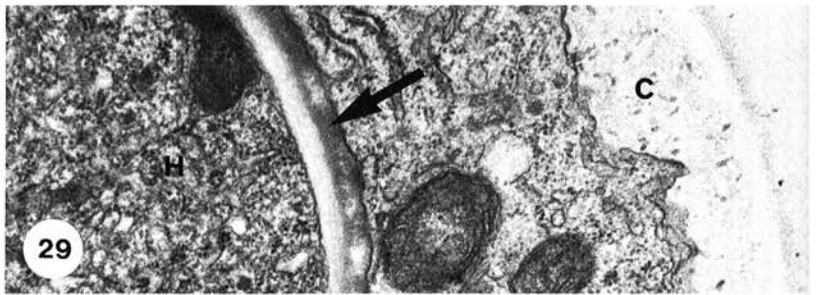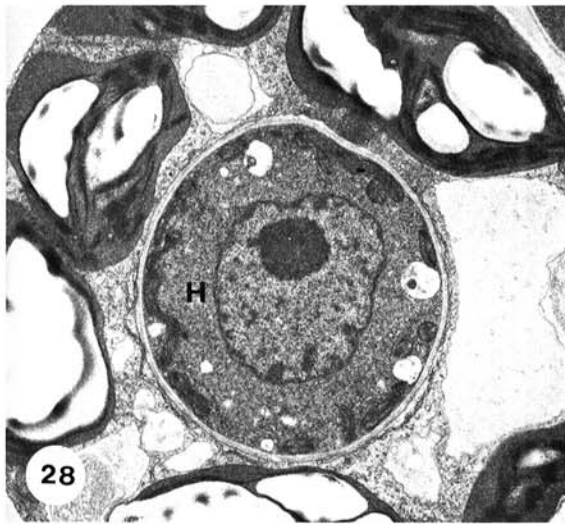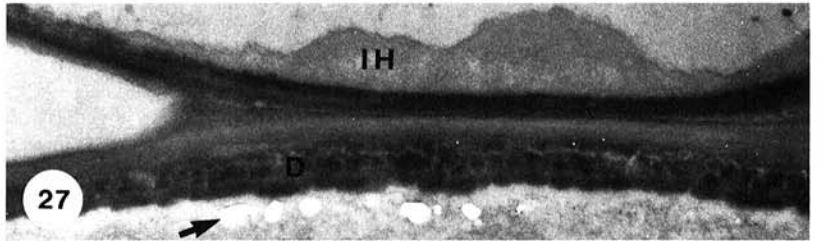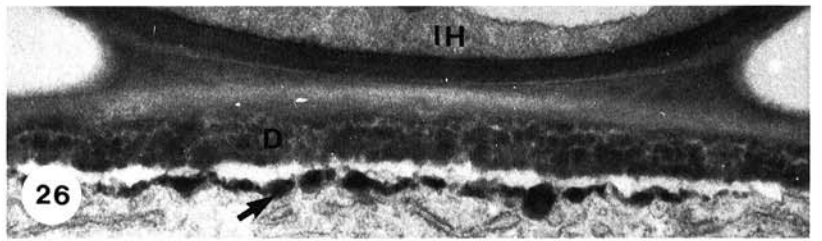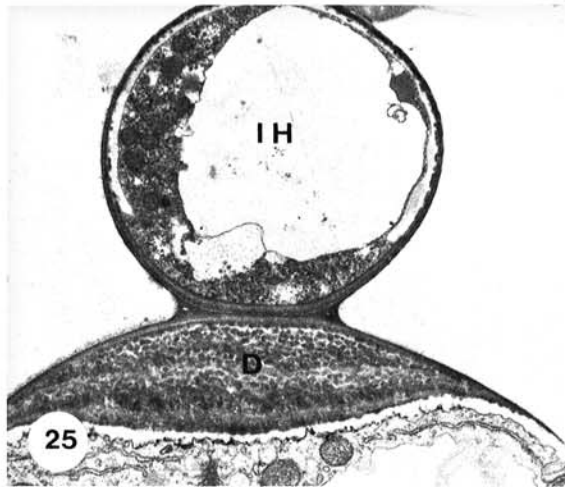
associated with lipid-like globules. At the two infection sites that were near veins, the neighboring xylem vessels were lined with electron-opaque material (Fig. 31). At one site only, the vacuole of an invaded, healthy plant cell contained electron-opaque material similar to the brittle material described below for polyoxin-treated tissue.

For tissue injected with polyoxin D, only sites with necrotic cells were chosen for examination by electron microscopy. In the two sites from tissue injected at 24 hr after inoculation, the infection hyphae were shriveled and contained disorganized, electron-opaque contents. Silica deposits were seen on and in adjacent mesophyll cell walls. In some sections where the infection hypha touched the plant wall, the fungus was embedded in material resembling fungal cell contents as described for the inhibitor-treated compatible interaction. Two large haustoria were present at both sites. At one, one haustorium was large, with disorganized cytoplasm and a thick wall (approximately 130 nm in width). The surrounding host cytoplasm was similarly disorganized and the plant cell was slightly collapsed. No extrahaustorium membrane could be distinguished, and the haustorium was separated from the host cytoplasm by an electron translucent space. Clumps of electron-opaque, apparently brittle material (the area tended to fracture during sectioning) was present in the cytoplasm (as in Fig. 32). The second haustorium was larger, lobed, and thicker walled (approximately 170–190 nm in width) and had vacuolate but otherwise fairly normal-looking cytoplasm (Fig. 33); that of the HMC also appeared normal. The EHM was 50–90 nm in width where it followed the contours of the haustorium, and contained granular material that was particularly conspicuous where the extrahaustorial membrane did not closely follow the haustorial wall (Figs. 33 and 34). Golgi bodies were unusually numerous in the neighboring host cytoplasm, which, in other respects, looked normal except that callose-like material lined the whole cell (Fig. 33) between the plasmalemma and the cell wall. About five collapsed, haustorium-lacking plant cells with disorganized cytoplasm were observed at this infection site, two of which were attached to the disorganized invaded cell. Adjacent, non-disorganized mesophyll cells had callose deposits between their plasmalemmas and cell walls where they were attached to necrotic cells. Electron-opaque material resembling silica was sometimes associated with these deposits in and adjacent to the plant wall. In these cases, the plasmalemma covering the deposits was associated with black, lipid-like globules as in (as in Fig. 32). Neighboring vessel elements were lined with electron-opaque, granular material not seen in uninfected areas of the leaf.

The second site also contained about five dead cells, but these were more collapsed and had darker, more uniform contents in which cellular structure was difficult to discern. Two large, lobed, and thick-walled (approximately 170 nm in width) haustoria were observed in one disorganized host cell (Fig. 32). Both haustoria and host cell closely resembled the necrotic haustorium and invaded cell described for the first site, as did the response of organized cells next to necrotic ones. A conspicuous difference between the two sites, however, was the greater abundance at the second site of silica deposits in such cells.

Two infection sites were examined in tissue treated with polyoxin D at 48 hr after inoculation. In both, the inhibitor appeared to have had a lesser effect than at the infection sites described above. The intercellular mycelium did not appear necrotic, and in terms of fungal or plant ultrastructure, neither of these infection sites appeared to differ significantly from the necrosis-containing sites examined in untreated tissue.

DISCUSSION

For rust fungi, bright yellow autofluorescence has been shown to be an indicator of fungal death (7); therefore, the present light microscope study suggests that both oxycarboxin and polyoxin D treatment killed the intercellular mycelium and the majority of haustoria in both susceptible and resistant plants soon after treatment. In susceptible plants, however, the most common response was the encasement of the haustorium in the absence of plant cell necrosis. Such an observation supports the conclusion from the previous study (7), in which the fungus was killed by heat, and that necrosis is not the inevitable, or the most common, consequence of fungal death.

The most significant difference between the effects of oxycarboxin and polyoxin D was the development of large, lobed, nonfluorescent haustoria in resistant and susceptible leaves treated with the latter. The similarity in appearance between these haustoria and those at the center of growing colonies in untreated plants suggests that they were alive and continuing to grow in spite of the inhibition or death of the intercellular infection hypha. The observation of such growing haustoria in the presence of a chitin synthesis inhibitor supports the conclusion from cytochemical data obtained for *Puccinia* species (1,2) that the walls of haustoria, but not intercellular mycelium, lack chitin. This conclusion was further supported by the present ultrastructural study, which indicated that haustorial wall synthesis continued in the presence of the inhibitor; haustorial walls were often unusually thick after polyoxin D treatment, except when the latter was applied close to the initiation of plant cell necrosis in the incompatible interaction.

The present experiments also confirm the previous conclusion (7) that killing the fungus 1 day, but not 2 days, after inoculation prevents the extensive necrosis that normally develops in the resistant cultivar 765. The results from the polyoxin D treatment given 1 day after inoculation indicate that although such necrosis usually did not develop at infection sites at which the haustorium was rapidly killed and encased, it commonly occurred when the haustorium remained alive. Such observations strongly indicate that the living haustorium is important for the induction of necrosis and that such induction occurs between 24–48 hr after inoculation. Because the majority of infection sites contained well-matured haustoria by 24 hr after inoculation, this induction of necrosis must have occurred some hours after the haustorium was fully formed. Treatment with polyoxin D also resulted in a slightly

←

Figs. 25–34. Electron micrographs of the incompatible interaction. **25–31,** Control plants harvested 4 or 5 d.p.i. **25,** Infection hypha (IH) adjacent to a mesophyll cell that has formed a large deposit (D) of silica-like material between the plasmalemma and the cell wall (× 9,002). **26,** An unstained, thick section of another deposit (D) next to the infection hypha (IH) shown in Figure 25. Note the electron-opaque material (arrow) on the plant plasmalemma (× 25,130). **27,** An unstained, thick section adjacent to that shown in Figure 26, which was treated with periodic acid. Note that the deposit (D) next to the infection hypha (IH) is still electron-opaque and that the material on the plant plasmalemma has been etched out (arrow) (× 25,130). **28,** A typical haustorium (H) formed by a growing colony at an infection site exhibiting no plant or fungus necrosis. Note that both haustorium and invaded cell look similar to those in the compatible interaction (c.f. Fig. 15) (× 6,331). **29,** An infection site with necrotic, uninvaded cells (not shown) and one ultrastructurally normal haustorium (H) in a plant cell that appears normal except for the callose-like material (C) lining the cell wall. The extrahaustorial matrix is wider than in the compatible interaction and contains electron-opaque material (arrow) (× 28,200). **30,** A haustorium (H) in a necrotic cell from an infection site with three haustoria only, one of which was in a nonnecrotic cell. Note that the haustorial cytoplasm appears to be at a lesser stage of disorganization than the host cytoplasm (× 8,200). **31,** Electron-opaque material (arrow) lining a xylem vessel near an infection site (× 22,000). **32–34,** Polyoxin D applied at 1 d.p.i., tissue harvested at 4 d.p.i. **32,** An infection site containing a single necrotic haustorium (H) in a necrotic cell. Note the dark material (arrow) in the plant cytoplasm and the electron-opaque material on the plasmalemma (arrow) next to a silica deposit in the adjacent nonnecrotic cell (× 3,620). **33,** An infection site containing one necrotic haustorium in a necrotic cell (not shown) and an apparently living, large haustorium (H) in a relatively normal-appearing cell. Note the granular material (arrow) in the extrahaustorial matrix between the haustorial lobes and the callose-like material (C) lining the plant wall. The areas of dark material outside the plant cell are the necrotic remains of the infection hypha (× 4,740). **34,** Electron-opaque material in the extrahaustorial matrix (EHM) and the thick haustorial wall (HW) surrounding the haustorium (H) shown in Figure 33 (× 34,900).

higher incidence of necrotic cells in resistant (Sr6) wheat leaves infected with *Puccinia graminis* f. sp. *tritici* than in comparable leaves given other fungus inhibitors (10); this difference similarly may have been due to the continued survival of the haustorium at some infection sites.

Both the light and electron microscope studies indicated that in the compatible interaction, fungal death or inhibition, before or after the formation of the first haustorium, did not result in the deposition of silica typically seen in older bean leaves (6) or when the plant responds to rust fungi pathogenic on other species (4,17,19). It would appear, therefore, that this response is not elicited by constitutive components of the dead or dying fungus. Nevertheless, such deposits were seen in the untreated incompatible cultivar; these occurred only rarely next to the infection hypha in control plants, but rather more frequently after polyoxin D treatment. Silica-containing deposits also were observed in living mesophyll cells where they contacted dead cells, although callose-like material also was present and was the more common component of such deposits. Significantly, the conspicuous lipid-like globules associated with the plant plasmalemma were observed only next to these silica-rich deposits; whether they are involved in silica deposition remains to be determined.

In the compatible interaction, electron microscopy revealed additional effects of polyoxin D treatment other than the increased frequency of necrotic haustoria and the presence of encasements similar to those described before (12). In particular, the extrahaustorial matrix often was unusually wide around nonnecrotic haustoria and contained more electron-opaque material than seen in control tissue. Such features often have been described in incompatible interactions with rust fungi (12), but were not reported after oxycarboxin treatment of a compatible bean-rust fungus interaction (15). More striking, however, was the fact that the plant cytoplasm adjacent to four out of the seven haustoria observed contained vesicles and tubules, some obviously in continuity with the extrahaustorial membrane, that closely resemble those reported previously during compatible interactions with *Puccinia* and *Melampsora* species (12), and *Physopella zeae* (8). However, such a response has not been seen (Heath, *unpublished*) or reported before for the compatible bean-rust system (12,14), even following oxycarboxin treatment (15), except in the one cell described in this study where the haustorium was slightly collapsed and had unusually dense contents. Whatever their role, these vesicles seem unlikely to be involved in the deposition of electron-opaque material in the extrahaustorial matrix, because they were not observed around haustoria in the incompatible interaction in which the matrix was much more clearly developed.

This absence of vesicles in the incompatible interaction, together with other characteristic ultrastructural features that were seen in polyoxin D treated and untreated resistant, but not susceptible, plants, further supports the conclusion (7) that inhibiting the fungus in a susceptible plant does not necessarily result in an incompatible-type interaction (as suggested in 11,15). In both treated and untreated leaves, the incompatible interaction was characterized by the cytoplasmic disorganization of haustoria and plant cells, thicker electron-opaque extrahaustorial matrices, and the lining of the cell wall of haustorium-containing cells with callose-like material. This last feature is particularly interesting because, to my knowledge, it has not been reported before in incompatible interactions with rust fungi. Callose deposition usually is considered to be the common result of membrane damage (9,18), and it is often observed, as in the present study, in

living cells at sites where they are attached to dead ones (12). However, the uniform nature of deposition in the invaded cell suggests that this was not a response to adjacent dead cells, nor was it a characteristic of dying cells lacking haustoria. The observations suggest, therefore, that the haustorium was in some way responsible for this uniform callose deposition and that this phenomenon may be related to the activity of the invaded cell that results in the death of the cells around it.

LITERATURE CITED

1. Chong, J., Harder, D. E., and Rohringer, R. 1981. Ontogeny of mono- and dikaryotic rust haustoria: Cytochemical and ultrastructural studies. Phytopathology 71:975-983.
2. Chong, J., Harder, D. E., and Rohringer, R. 1986. Cytochemical studies on *Puccinia graminis* f. sp. *tritici* in a compatible wheat host. II. Haustorium mother cell walls at the host cell penetration site, haustorial walls, and the extrahaustorial matrix. Can. J. Bot. 64:2561-2575.
3. Endo, A., and Misato, T. 1969. Polyoxin D, a competitive inhibitor of UDP-N-acetylglucosamine:chitin N-acetylglucosaminyltransferase in *Neurospora crassa*. Biochem. Biophys. Res. Com. 37:718-722.
4. Heath, M. C. 1979. Partial characterization of the electron-opaque deposits formed in the non-host plant, French bean, after cowpea rust infection. Physiol. Plant Pathol.15:141-148.
5. Heath, M. C. 1980. Effects of infection by compatible species or injection of tissue extracts on the susceptibility of nonhost plants to rust fungi. Phytopathology 70:356-360.
6. Heath, M. C. 1981. The suppression of the development of silicon-containing deposits in French bean leaves by exudates of the bean rust fungus and extracts from bean rust-infected tissue. Physiol. Plant Pathol. 18:149-155.
7. Heath, M. C. 1984. Relationship between heat-induced fungal death and plant necrosis in compatible and incompatible interactions involving the bean and cowpea rust fungi. Phytopathology 74:1370-1376.
8. Heath, M. C., and Bonde, M. R. 1983. Ultrastructural observations of the rust fungus *Physopella zeae* in *Zea mays*. Can. J. Bot. 61:2231-2242.
9. Kauss, H. 1987. Some aspects of calcium-dependent regulation in plant metabolism. Annu. Rev. Plant Physiol. 38:47-72.
10. Kim, W. K., Rohringer, R., Samborski, D. J., and Howes, N. K. 1977. Effect of blasticidin S, ethionine, and polyoxin D on stem rust development and host-cell necrosis in wheat near-isogenic for gene Sr6. Can. J. Bot. 55:568-573.
11. Kiraly, Z., Barna, B., and Ersek, T. 1972. Hypersensitivity as a consequence, not the cause, of plant resistance to infection. Nature (London) 239:456-458.
12. Littlefield, L. J., and Heath, M. C. 1979. Ultrastructure of Rust Fungi. Academic Press, New York. 277 pp.
13. Madden, L. V., Knoke, J. K., and Louie, R. 1982. Considerations for the use of multiple comparison procedures in phytopathological investigations. Phytopathology 72:1015-1017.
14. Pring, R. J. 1980. A fine-structural study of the infection of leaves of *Phaseolus vulgaris* by uredospores of *Uromyces phaseoli*. Physiol. Plant Pathol. 17:269-276.
15. Pring, R. J., and Richmond, D. V. 1976. An ultrastructural study of the effect of oxycarboxin on *Uromyces phaseoli* infecting leaves of *Phaseolus vulgaris*. Physiol. Plant Pathol. 8:155-162.
16. Sokal, R. R., and Rohlf, F. J. 1981. Biometry. W. H. Freeman and Company, San Francisco. 859 pp.
17. Stumpf, M. A., and Heath, M. C. 1985. Cytological studies of the interactions between the cowpea rust fungus and silicon-depleted French bean plants. Physiol. Plant Pathol. 27:369-385.
18. Wheeler, H. 1974. Cell wall and plasmalemma modifications in diseased and injured plant tissues. Can. J. Bot. 52:1005-1009.
19. Wood, L. A. and Heath, M. C. 1986. Light and electron microscopy of the interaction between the sunflower rust fungus (*Puccinia helianthi*) and leaves of the nonhost plant, French bean (*Phaseolus vulgaris*). Can. J. Bot. 64:2476-2486.